

Perspective

Chemically Functionalized 2D Transition Metal Dichalcogenides for Sensors

Selene Acosta ^{1,*} and Mildred Quintana ^{1,2}

¹ Centro de Investigación en Ciencias de la Salud y Biomedicina, Universidad Autónoma de San Luis Potosí, Av. Sierra Leona 550, Lomas de San Luis, San Luis Potosí 78210, Mexico; mildred.quintana@uaslp.mx

² Facultad de Ciencias, Universidad Autónoma de San Luis Potosí, Av. Parque Chapultepec 1570, Privadas del Pedregal, San Luis Potosí 78295, Mexico

* Correspondence: selene.acosta@uaslp.mx

Abstract: The goal of the sensor industry is to develop innovative, energy-efficient, and reliable devices to detect molecules relevant to economically important sectors such as clinical diagnoses, environmental monitoring, food safety, and wearables. The current demand for portable, fast, sensitive, and high-throughput platforms to detect a plethora of new analytes is continuously increasing. The 2D transition metal dichalcogenides (2D-TMDs) are excellent candidates to fully meet the stringent demands in the sensor industry; 2D-TMDs properties, such as atomic thickness, large surface area, and tailored electrical conductivity, match those descriptions of active sensor materials. However, the detection capability of 2D-TMDs is limited by their intrinsic tendency to aggregate and settle, which reduces the surface area available for detection, in addition to the weak interactions that pristine 2D-TMDs normally exhibit with analytes. Chemical functionalization has been proposed as a consensus solution to these limitations. Tailored surface modification of 2D-TMDs, either by covalent functionalization, non-covalent functionalization, or a mixture of both, allows for improved specificity of the surface–analyte interaction while reducing van der Waals forces between 2D-TMDs avoiding agglomeration and precipitation. From this perspective, we review the recent advances in improving the detection of biomolecules, heavy metals, and gases using chemically functionalized 2D-TMDs. Covalent and non-covalent functionalized 2D-TMDs are commonly used for the detection of biomolecules and metals, while 2D-TMDs functionalized with metal nanoparticles are used for gas and Raman sensors. Finally, we describe the limitations and further strategies that might pave the way for miniaturized, flexible, smart, and low-cost sensing devices.



Citation: Acosta, S.; Quintana, M. Chemically Functionalized 2D Transition Metal Dichalcogenides for Sensors. *Sensors* **2024**, *24*, 1817. <https://doi.org/10.3390/s24061817>

Academic Editor: Dimitris Tsoukalas

Received: 8 February 2024

Revised: 6 March 2024

Accepted: 11 March 2024

Published: 12 March 2024



Copyright: © 2024 by the authors. Licensee MDPI, Basel, Switzerland. This article is an open access article distributed under the terms and conditions of the Creative Commons Attribution (CC BY) license (<https://creativecommons.org/licenses/by/4.0/>).

Keywords: chemical sensors; 2D transition metal dichalcogenides; chemical functionalization; biosensors; gas sensors; metal sensors; Raman sensors

1. Introduction

The development of chemical sensors focuses on the design of cost-effective and reliable devices for detecting and measuring individual chemical compounds in relevant environments. Today, chemical sensors are found in every industry, for example, in food and beverage, agriculture, environmental conservation, mining, automotive, healthcare, packing, transportation, etc. [1–4]. With the increasing demand for sensors, there is a need for novel portable platforms for the detection of new analytes exhibiting high selectivity and sensitivity, low power consumption, chemical and mechanical stability, and to be accessible to all people.

The 2D materials graphene, hexagonal boron nitride (h-BN), TMDs, graphitic carbon nitrides (g-C₃N₄), layered metal oxides, black phosphorus (BP), and MXenes are excellent materials to fully meet these requirements [5–7]. The remarkable properties of 2D materials arise from electron confinement in two dimensions, the absence of strong interlayer interactions and atomic thickness, which results in a high surface area. Applicability of

2D materials in sensors depends on factors such as sheet thickness, the chemical nature of the pristine material, surface composition, and defects. Individual layers of 2D materials display significant changes in their properties compared to their bulk counterparts. For instance, the bandgap of the TMD MoS₂ shifts from indirect to direct when a single sheet is isolated, leading to fluorescence in MoS₂ [8]. Consequently, MoS₂ is well-suited for optoelectronic applications, including photodetectors, electroluminescence, and luminescent probes. Extensive research has been guided using 2D materials for sensing applications due to the numerous advantages offered by their two-dimensional structure in devices [9–11]. The atomic thickness of 2D materials allows for the direct interaction between all atoms in the material and the analyte. Their large area not only ensures a significant active surface for sensing but also simplifies device assembly, and their unique electronic and optical properties, combined with their surface chemistry and structure, enable their interaction with specific targets, including gases, metals, and biological molecules [12–16].

For the implementation of 2D materials as sensors, there must be an interaction between the surface of the 2D material and the analyte, resulting in a measurable change in either the properties of the 2D material or the analyte itself. This interaction can be categorized as either covalent or non-covalent, depending on the chemical characteristics of the analyte and the 2D material. For example, graphene primarily undergoes interactions such as hydrogen- π , π - π , cation- π , and anion- π interactions due to its π electron system [17–19]. Interactions between 2D-TMDs and analytes are typically electrostatic and van der Waals interactions, while covalent interactions involve chemical reactions between analytes and 2D materials to form covalent bonds on their basal planes, a process known as chemical adsorption. Conversely, non-covalent interactions involve the physical adsorption of analytes onto the basal planes of 2D material sheets [5,20].

The tailored design and production of the optimal molecular interaction depend on the required type of sensor. If the sensing mechanism involves immediate response and rapid recovery, physical adsorption is preferred. However, if biological analytes are to be immobilized on the surface of the 2D material, only chemical adsorption can provide the required stability. For chemical and physical adsorption, the use of pristine 2D materials in sensors often does not result in the highest sensitivities and selectivity [21–23]. The primary drawback is linked to the weak interaction that pristine 2D materials exhibit with analytes. For 2D-TMDs, these interactions occur as van der Waals interactions, which are indeed extremely weak forces. Dangling bonds on 2D-TMDs facilitate strong and specific interactions with analytes. Other limitations of 2D materials include agglomeration and settling in dispersion, reducing the sensing surface area. To address these disadvantages, surface modification of 2D-TMD materials has been successfully performed through defect creation or functionalization, enhancing the interaction between 2D-TMDs and specific analytes [24–27].

From this perspective, we focus on the use of TMDs as sensor platforms as they are, so far, the most studied 2D materials after graphene and graphene oxide, particularly MoS₂. TMDs follow the chemical formula MX₂ in their structure. M is a transition metal, and X is a chalcogen. Forty different TMDs have been reported; among them, the most studied are MoS₂, WS₂, WSe₂, and MoSe₂ [7]. A single layer of TMDs comprises three atomic stratum linked through covalent bonds, with the transition metal positioned between two chalcogens. In bulk, TMDs are layered materials whose layers are attached by van der Waals interactions. Monolayers of TMDs have astonishing properties due to the confining of charge carriers in two dimensions. These properties convert them into potential materials for chemical sensors. The d orbitals in the electronic structure of 2D-TMDs allow us to adjust their physical properties as valence electrons, carrier mobility, and chemical and mechanical stability. The 2D-TMDs have been extensively investigated for chemical sensing applications due to their high area-to-volume ratio. In most of the reported works, 2D-TMD nanosheets are obtained via chemical and liquid phase exfoliation. The 2D-TMDs obtained through chemical exfoliation processes have limitations that hinder their use in sensors; these limitations include agglomeration and settling when the nanosheets are

in dispersion and a deficiency of dangling bonds to facilitate the covalent conjugation of external probes. These drawbacks can be easily tackled by means of 2D-TMDs surface functionalization, a process that can be accomplished by utilizing 2D-TMDs defects, such as chalcogen vacancies, produced during exfoliation processes.

As is widely known, the synthetic methodology used to produce 2D-TMDs influences the structural defects present in the materials. The 2D-TMDs obtained through chemical and liquid phase exfoliation tend to be rich in chalcogen vacancies [28]. The defects in 2D-TMDs dictate their surface properties and, consequently, their ability to interact with molecules. While defects may pose disadvantages in certain applications, such as optoelectronics, carefully engineered defects can introduce new and adjustable properties for applications in sensor devices. Modifying pristine 2D-TMDs to adjust their properties and improve their interaction with analytes is achieved through chemical functionalization. Functionalization involves altering the surface properties of a material by introducing or attaching chemical groups or molecules. The enhanced sensing of 2D-TMDs through functionalization has been pursued using various approaches. The 2D-TMDs are functionalized in both covalent and non-covalent protocols with molecules and biomolecules such as DNA, RNA, proteins, polymers, and nanoparticles.

Herein, we provide a summary and discussion of the recent advancements in both covalent and non-covalent functionalization of 2D-TMDs with the aim of enhancing their efficiency as chemical sensors towards different analytes. This perspective specifically focused on highlighting how surface modification of 2D-TMDs allows for tuning their properties, leading to the development of chemical sensors characterized by increased sensitivity, selectivity, and low detection limits. Biosensors, metal sensors, gas sensors, and Raman sensors are described. We further describe some strategies that might pave the way for miniaturized flexible, smart, and low-cost sensing devices. To the best of our knowledge, this is the first perspective exclusively dedicated to the chemical functionalization of 2D-TMDs for chemical sensors.

2. Biosensors

MoS₂ is the most studied of the 2D-TMDs due to its physicochemical properties like large band gap, flexibility, and photoluminescence. One of the first works of functionalized MoS₂ used for chemical sensing was reported by Huang and collaborators in 2013 [29], where MoS₂ sheets obtained from sonication were functionalized with Cu nanoparticles by directly performing a chemical reduction of a copper chloride onto MoS₂ nanosheets using glucose and 1-hexadecylamine. Large area MoS₂ nanosheets decorated with well-distributed copper nanoparticles with diameters up to 5 nm were obtained. Afterward, the synthesized material was evaluated in glucose sensing by depositing Cu-MoS₂ in a glassy carbon electrode and using cyclic voltammetry and amperometry to seek the oxidation of glucose by Cu-MoS₂. The Cu-MoS₂ sensor exhibited a sensitivity of 1055 $\mu\text{A mM}^{-1} \text{cm}^{-2}$ and selectivity upon ascorbic acid, uric acid, and dopamine.

MoS₂ had been functionalized with different biomolecules to produce biosensors. A widely explored strategy is the functionalization of MoS₂ with DNA. In 2014, Mei Kong et al. [30] developed a biosensor based on MoS₂ obtained by lithium intercalation; the nanosheets exhibit a wrinkled paper-like structure. Afterward, MoS₂ was non-covalently functionalized with a dye-labeled single-stranded DNA probe (aptamer). The DNA-MoS₂ interaction occurs through van der Waals forces between the nucleobases and the basal plane of MoS₂ nanosheets. In this report, the aptamer recognized the prostate-specific antigen (PSA), a biomarker used for the diagnosis of prostate cancer. The functionalization of MoS₂ with the aptamer induced an aptamer fluorescence quenching. The sensor device was developed using the aptamer fluorescence as a transducer signal; the fluorescence of the aptamer was recuperated as it bonded with PSA and liberated from MoS₂. This sensor had a 0.2 ng/mL detection limit and worked in human serum samples. An analogous work was reported by Zhang and collaborators in 2021 [31], where PSA was detected with a field-effect transistor biosensor device based on a DNA tetrahedron functionalized MoS₂

followed by a functionalization with the protein biotin–anti-PSA. In this work, the authors achieved a detection limit of 1 fg/mL. This impressive result was related to the stable immobilization provided by the DNA-MoS₂ functionalization. Following a similar strategy, Chun Lin and collaborators [32] fabricated a biosensor based on MoS₂ functionalized with an aptamer to detect thrombin, a biomolecule used to monitor inflammation. MoS₂ nanosheets were obtained through liquid-phase exfoliation. The sensor platform was made of SiO₂ substrates where Pt electrodes were deposited using an e-beam cryo-evaporator, and MoS₂ nanosheets were subsequently deposited on the electrode having sizes up to 100 nm (Figure 1B). The aptamer was immobilized on the surface of MoS₂ by incubation at room temperature for 90 min. Their interaction was confirmed by impedance measurements, and it is based on van der Waals interactions. The detection of thrombin was made by monitoring changes in impedance resulting from the interactions between the immobilized aptamer on the electrode surface and thrombin (Figure 1A). The sensor was capable of quantifying thrombin in human serum.

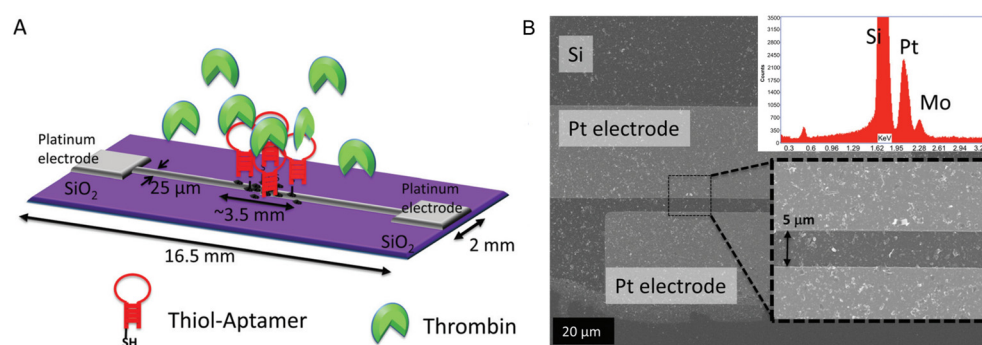


Figure 1. (A) Schematic representation of a thrombin biosensor based on aptamer functionalized MoS₂. (B) SEM image of MoS₂ deposited on a Pt electrode. The inset displays Energy Dispersive X-ray (EDAX) spectra from the zone in the square of SEM micrography. Adapted from [32].

The defects produced in MoS₂ sheets during their synthesis can be used to assist their functionalization. Behera and collaborators [33] used the sulfur vacancies produced in MoS₂ during exfoliation to functionalize MoS₂ nanosheets with different cationic thiol ligands. MoS₂ nanosheets exhibit a diameter range of 300–600 nm and a height of approximately 1.2 nm. The positive charge induced through thiol functionalization allowed the conjugation of MoS₂ with the fluorescent protein GFP, which has a negative charge; the conjugation of GFP with functionalized MoS₂ induced a quenching in the GFP fluorescence. Afterward, a biosensor was developed based on a displacement assay of GFP with several analytes competing for the interaction with functionalized MoS₂. The release of GFP from functionalized MoS₂ incited the recovery of the fluorescence (Figure 2). In this report, GFP fluorescence was used as the signal transducer to detect 15 different proteins, such as β -galactosidase and macerozyme.

The functionalization during the synthesis of MoS₂ was explored by Xu and collaborators [34]. In this report, MoS₂ was functionalized with thioglycolic acid (TGA) through a hydrothermal treatment where molybdenyl acetylacetonate, TGA, and sodium sulfide were the precursors, and the product of this synthesis was TGA-MoS₂ nanosheets. The MoS₂ nanosheets exhibit curling and overlapping due to their ultrathin characteristics and TGA surface modification (Figure 3A). The average thickness of the MoS₂ nanosheets obtained by AFM confirmed the production of single-layer nanosheets. Additionally, TGA-MoS₂ presented a fluorescence centered at 420 nm, with intensity decreased in the presence of dopamine (Figure 3B,C). Xu and colleagues reported a facile method where dopamine can be sensed using the fluorescence of TGA-MoS₂ as a transducing signal, achieving a detection limit of 27 nM.

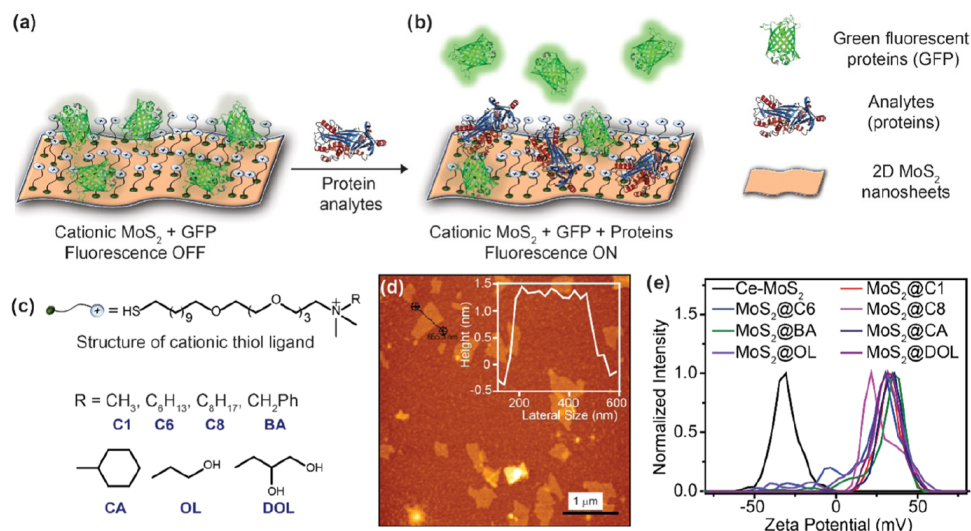


Figure 2. (a) Schematic representation of the sensor developed by Behera et al. Quenching of GFP fluorescence by cationic MoS₂. (b) Addition of the analyte releases GFP from the surface of cationic MoS₂, followed by regeneration of GFP fluorescence. (c) Structure of cationic thiol ligands. (d) Atomic force microscopy (AFM) image of chemical exfoliated MoS₂ (Ce-MoS₂). (e) ζ -Potential plot for MoS₂ that proves thiol functionalization. Reproduced from [33].

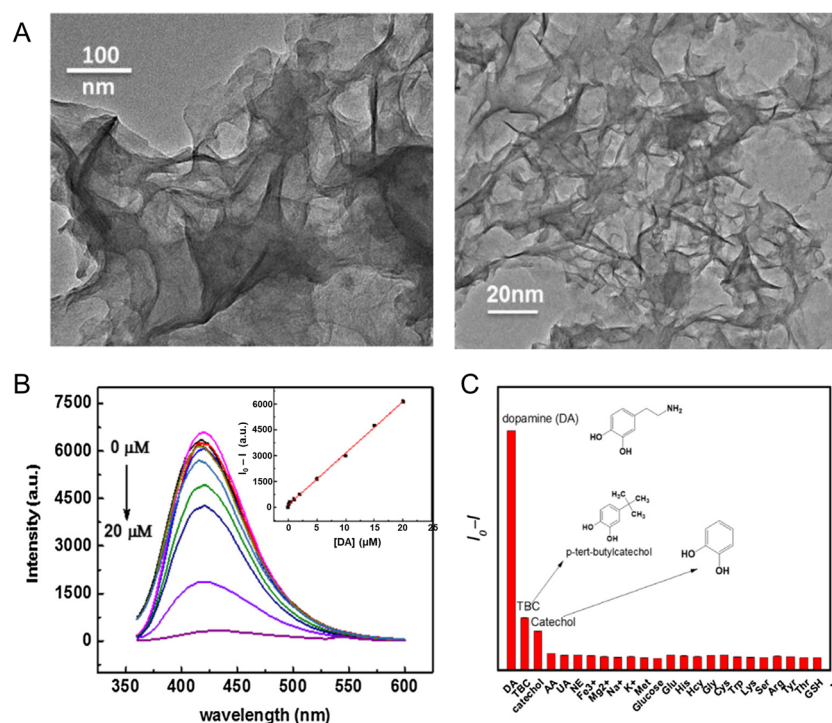


Figure 3. (A) TEM images of the TGA-MoS₂ nanosheets. (B) Fluorescence emission spectra recorded for the TGA-MoS₂ sensor at various concentrations of dopamine. Inset: standard curve established to determine the concentration of dopamine. (C) Fluorescence response of TGA-MoS₂ with different guest molecules. Reproduced from [34].

Guo and collaborators [35] functionalized MoS₂ nanosheets with thiourea via a microwave-assisted hydrothermal route. Nanosheets with lateral size range from 200 to 300 nm were reported. The change in the interlayer spacing from 0.62 nm in pristine MoS₂ to 0.92 nm in thiourea-MoS₂, observed in high-resolution transmission electron microscopy (HR-TEM) images, is evidence of MoS₂ functionalization. Afterward, a biosensor was constructed using the amino group in thiourea to attach an antigen named GE11, which

recognizes the EGFR receptor present in human liver cancer cells. The biosensor was developed by measuring the change in the impedance as a function of cell concentration, allowing a low detection limit of 50 cells/mL (Figure 4).

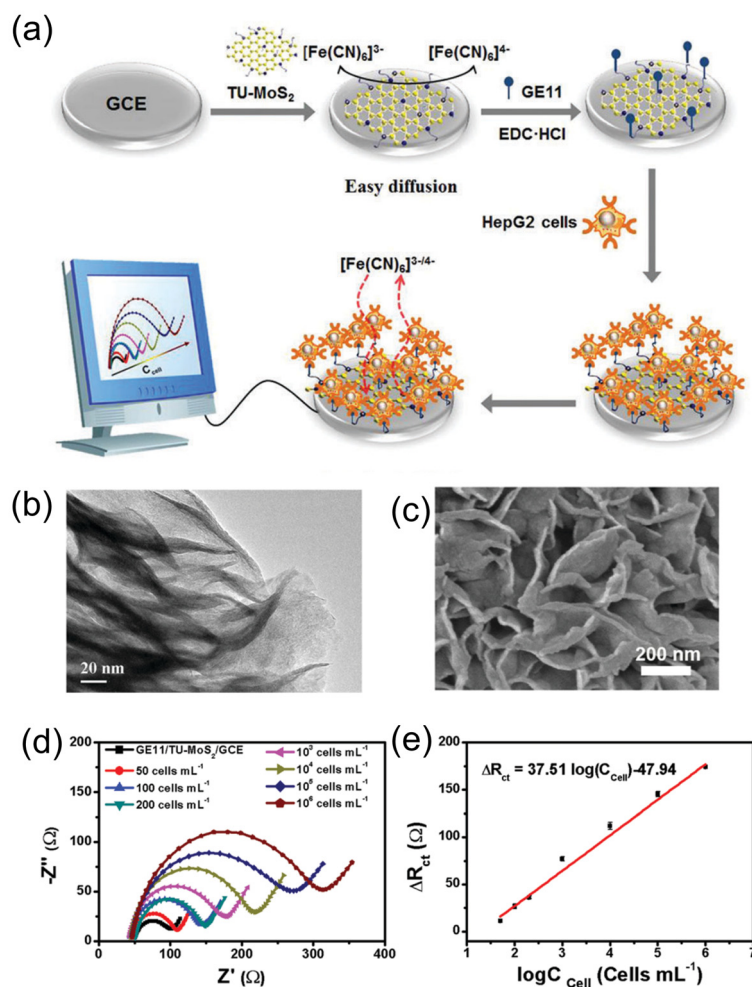


Figure 4. (a) Schematic illustration for fabrication of biosensor based on surface functionalized thiourea-MoS₂ nanosheets. (b) TEM image of thiourea-MoS₂ nanosheets. (c) SEM image of thiourea-MoS₂ nanosheets. (d) Electrochemical impedance spectroscopy (EIS) response of GE11/TU-MoS₂ electrode to various concentrations of HepG2 cells. (e) Calibration curve of ΔR_{ct} vs. $\log C_{cell}$. Adapted from [35].

Singh and collaborators [36] functionalized MoS₂ with cetyltrimethyl ammonium bromide (CTAB) by sonicating MoS₂ powder in water with CTAB (1%) solution to accomplish the conjugation of an antibody that recognized the microorganism *Salmonella typhimurium* in a microfluidics electrode. Transmission electron microscopy (TEM) analysis showed the obtention of CTAB-MoS₂ nanosheets with lateral sizes ranging from 50 to 200 nm. The observation of single MoS₂ layers indicates that CTAB can efficiently assist in the exfoliation of MoS₂ in water. Additionally, SEM analysis showed that CTAB-MoS₂ are mostly arranged in a flower-like structure. *S. typhimurium* is a Gram-negative bacterium responsible for a great part of human food poisoning in the world. Singh reports on a microfluidic immunosensor utilizing electrochemical impedance spectroscopy for the detection of *S. typhimurium* with a sensitivity of 1.79 kΩ/CFU⁻¹ mL cm⁻². Zhang and collaborators [37] developed an electrochemical sensor toward the PIK3CA gene, which is associated with lung cancer. The sensor was based on MoS₂ nanosheets functionalized with riboflavin 5'-monophosphate sodium salt (FMS); the functionalization was carried out during the synthesis of MoS₂ through liquid-phase exfoliation. FMS-functionalized MoS₂ has wrinkly layered structures and was successfully dispersed in water, contrary to pristine MoS₂, in which agglomeration

was observed in SEM images. To fabricate the sensor, FMS-MoS₂ nanosheets were deposited on a glassy carbon electrode, and a ssDNA was bonded covalently to the FMS-MoS₂ using the amine groups of the ssDNA and the phosphonate groups of the FMNs. The ssDNA was complementary to the PIK3CA gene, and cyclic voltammograms were measured when the sensor was in the presence and absence of the PIK3CA gene.

Even though most of the sensors based on MoS₂ functionalized with metal nanoparticles had been studied for the detection of toxic and hazardous gases, these materials may also work for the detection of other kinds of molecules [38,39]. For example, Wang et al. [40] synthesized MoS₂ functionalized with Au-nanoparticles and used it for the construction of a DNA sensor based on electrochemiluminescence. SEM characterization showed a smooth and large surface area of the produced MoS₂ nanosheets and Au-nanoparticles with 13 nm in diameter that were well dispersed in the surface of MoS₂. The sensor was developed in a sandwich type where Au-MoS₂ were functionalized with DNA as well as CdS/ZnS quantum dots coated with polyethyleneimine. The QDs were attached to the DNA that was going to be detected and Au-MoS₂ to a reporter DNA. This sensor can detect DNA at a concentration of 0.05–1000 fM. Different types of nanoparticles have been used to functionalize MoS₂ and increase its sensing performance. In 2021, Xiao et al. [41] deposited MoS₂ nanosheets in a screen-printed electrode and grew Au-Pt nanoparticles onto the MoS₂ surface using electrodeposition. The morphology of the electrode was characterized using SEM, and a clear difference was observed in the electrode with and without Au-Pt MoS₂ functionalization. The bare electrode was smoother than the functionalized one. Au-Pt nanoparticles had a diameter ranging from 110 to 130 nm. The fabricated sensor was used to detect lactic acid, a metabolite used as a biomarker in medical diagnosis. Au-Pt-NPs functionalization increased the electron transfer rate and worked as an oxidant of lactic acid in the sensing reaction.

The co-functionalization of MoS₂ nanosheets with a thiol end molecule and metal nanoparticles for the development of an RNA biosensor was explored by Zhu and collaborators [42]. In this report, the synthesis of the MoS₂-Thi-AuNPs nanocomposite was achieved through a microwave-assisted hydrothermal method, followed by assembly onto a glassy carbon electrode. TEM characterization showed the few layers of exfoliation of MoS₂ and the formation of Au-nanoparticles on their surface with an average diameter of 40 nm. DNA conjugation was used as a recognition probe, and thionine acted as an electrochemical indicator for the detection of RNA and as a reducing agent for the formation of Au-nanoparticles (Figure 5). This sensor device was able to detect RNA with a limit detection of 0.26 pM and the possibility of detecting specific RNA in human serum.

Emerging viruses, such as COVID-19, responsible for the pandemic that emerged in 2019 in Wuhan, China, highlighted the importance of the fast and simple development of innovative biosensors. The 2D materials properties allowed the fabrication of COVID-19 biosensors with high sensitivity [43]. Peng and collaborators [44] used carboxyl functionalized MoS₂ deposited on ITO to identify SARS-CoV-2 and its S protein by n-IR plasmonic response at 1550 nm. The linear detection range for the SARS-CoV-2 ranged from 0 to 67.87 nM, and its S glycoprotein was between 0 and 301.61 nM.

The functionalization of other 2D-TMDs and their application in different biosensors has also been investigated. The functionalization of WS₂ with the porphyrin hemin was reported by Chen and collaborators [45]. The functionalization was confirmed by UV-vis absorption spectra and X-ray photoelectron spectroscopy (XPS); SEM characterization showed the layered structure of hemin-WS₂, indicating that functionalizing WS₂ with hemin does not affect its prime structure. The interaction between WS₂ and hemin was carried out through van der Waals interactions. The hemin-WS₂ nanosheets presented peroxidase-like activity, and the oxidation of a substrate produced a colored reaction. Chen and colleagues used this colored reaction to develop a simple glucose sensor using glucose oxidase and the hemin-functionalized WS₂. The glucose sensor reported in this work had a detection limit of 1.5×10^{-6} mol L⁻¹. This sensor can be considered low-cost production as it is based on a colorimetric reaction easily detected by the naked eye. Yang et al. [46]

functionalized WS₂ nanosheets with a modified polymer to develop a biosensor of glycosylated hemoglobin. The polymer used was boronic acid-modified polyvinyl alcohol (B-PVA), and WS₂ nanosheets were functionalized with it during their liquid-phase exfoliation. TEM images of the B-PVA-WS₂ nanosheets revealed a clearly defined thin 2D structure featuring a lateral size of approximately 50 nm. The electron diffraction pattern of the B-PVA-WS₂ demonstrates their inherent 2H phase following exfoliation and functionalization with B-PVA. B-PVA-WS₂ presented intense fluorescence when excited at 532 nm, and its fluorescence was quenched in the presence of glycosylated hemoglobin. The sensor was developed using the B-PVA-WS₂ fluorescence intensity and detected glycosylated hemoglobin down to the concentration 3.3×10^{-8} M (Figure 6).

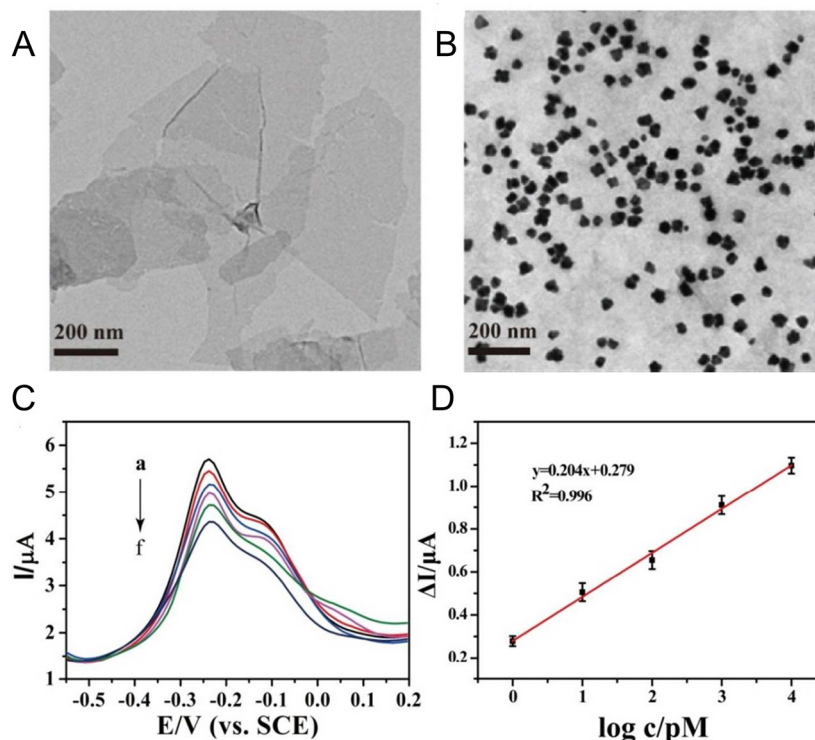


Figure 5. (A) Transmission electron microscopy of WS₂ and (B) MoS₂-Thi-AuNPs nanocomposite. (C) MoS₂-Thi-AuNPs response to numerous miR-21 concentrations (a–f: 0, 1.0, 10, 100, 1000 and 10,000 pM). (D) Calibration curves of sensor responses to miR-21. Adapted from [42].

Luo et al. [47] reported MoSe₂ nanosheets that were synthesized hydrothermally and treated with Ar plasma to induce selenium vacancies. Additionally, nitrogen atoms were introduced to the vacancies through N₂ plasma. The morphological change of MoSe₂ during plasma functionalization was monitored through SEM. Prior to functionalization, MoSe₂ presented a smooth layered structure with an average lateral size of 60 nm; after plasma treatment, the surface of MoSe₂ was rough and there was a mutilation of the edges. The presence of Nitrogen functionalization and Se vacancies were observed by HRTEM and EDS analysis. Afterward, N-MoSe₂ nanosheets were deposited on a glassy carbon electrode to evaluate its sensing performance towards H₂O₂. The sensor developed by Luo demonstrated effective performance in detecting hydrogen peroxide, boasting a low detection limit of 12.6 nmol/L. Finally, in a recent work reported by Song et al. [48], fluorinated WSe₂ nanosheets (F-WSe₂) were used to develop an efficient platform for detecting cytosolic miRNA. The morphological properties of fluorinated WSe₂ nanosheets were characterized through TEM and AFM. F-WSe₂ had an average particle size of 120 nm and an average thickness of 1.1 nm; this was evidence of the obtention of single-layer F-Wse₂. To fabricate a sensor device, a fluorophore-labeled single-stranded DNA (ssDNA) was adhered to the F-WSe₂ nanosheet surface through electrostatic interaction and π - π stacking. This bonding resulted in a significant quenching of the ssDNA fluorescence.

The formation of double-stranded complexes occurs as single-stranded DNA (ssDNA) hybridizes with its target in the cytosol. Consequently, the target strand was released from the surface of F-WSe₂, allowing the retention of probe fluorescence. Successful detection of intracellular miRNA-21 and miRNA-210 was achieved with this novel sensor. In this work, it was reported for the first time the cytosolic delivery of 2D nanomaterials.

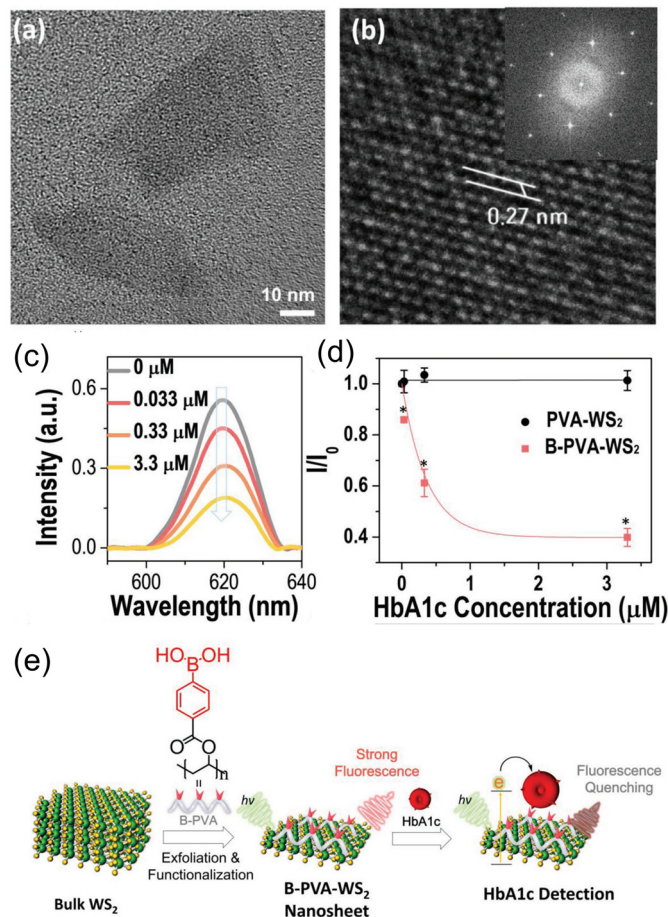


Figure 6. (a) TEM of B-PVA-WS₂ nanosheets. (b) HRTEM image of B-PVA-WS₂. (c) Photoluminescence spectra of B-PVA-WS₂ at various concentrations of glycated hemoglobin. (d) Assessment of photoluminescence quenching responses between PVA-WS₂ (non boronic acid present) and B-PVA-WS₂ in the presence of glycated hemoglobin. * $p < 0.001$ versus negative control. (e) Schematic diagram of biosensor developed by Yang and collaborators. Adapted from [46].

3. Metal Sensors

The sensing of extremely low concentrations of heavy metals in water is crucial for environmental care. In 2018, Gan and collaborators [49] searched for an MoS₂ functionalization that allowed for the change in the electronic surface of MoS₂ nanosheets without changing their original lattice structure. To achieve this, MoS₂ was exfoliated with N, N-dimethylformamide (DMF), 1-methyl-2-pyrrolidinone, and formamide, expecting to induce nitrogen functionalities on the MoS₂ nanosheets. AFM analysis indicated that MoS₂ was obtained as nine-, five-, and eleven-layered materials depending on the solvent used. In addition, TEM analysis showed that MoS₂ exfoliated with formamide results in the smaller MoS₂ nanosheets obtained. Through DFT calculations, Gan and collaborators probed that Mo-N covalent bonds can be formed between MoS₂ nanosheets and the nitrogen atoms present in the solvent molecules. The N-MoS₂ functionalized surfaces were then deposited on a glass carbon electrode and used to detect Cd²⁺ from water with a detection limit of 0.2 nM. In the same research direction, Bazylewski et al. [50] developed a Cd²⁺ sensor based on L-cysteine functionalized MoS₂. First, MoS₂ nanosheets were obtained

from ultrasonication in a mix of thioglycolic acid and water to obtain carboxylated MoS₂ (COOH-MoS₂). Afterward, the carboxyl group was used in an amide cross-linking reaction to attach L-cysteine to MoS₂ nanosheets. Thin films of Cys-MoS₂ were assembled by vacuum filtration using poly(ether)sulfone as support. SEM analysis of the obtained films showed that MoS₂ nanosheets tend to form clusters with a thickness ranging from 100 nm to 2 μm. More uniform films were observed in the presence of L-cysteine as a result of cross-linking induced by cysteine. The Cys-MoS₂ films were integrated into a chemiresistor whose resistivity increased in contact with water containing 5 ppb of Cd²⁺. The device developed by Bazylewski and collaborators operated in a range of 1–500 ppb and was selective for Cd²⁺ detection.

The sensing of silver ions had been performed using a biosensor based on functionalized MoS₂. Pal and collaborators [51] functionalized MoS₂ with carboxyl groups by sonication with potassium hydroxide and monochloroacetic acid in deionized water. FESEM was used to analyze the layered structure of functionalized MoS₂ and Raman spectroscopy to prove the COOH-functionalization of MoS₂. XRD showed that after functionalization, MoS₂ nanosheets conserve their regular hexagonal 2H polycrystalline crystal structure. Afterward, the carboxyl-MoS₂ nanosheets were attached to a gold working electrode and functionalized with a poly(cytosine) oligonucleotide comprising 20 bases. The sensing of Ag⁺ ions was achieved by exploiting the conjugation between cytosine and Ag⁺ (cytosine-Ag(I)-cytosine). The sensing was carried out by dipping the fabricated electrode in Ag⁺-containing solutions and using the square wave voltammetry (SWV) method (Figure 7). The Ag⁺ sensor device reported by Pal et al. had a limit of detection of 0.8 pM in potable water, which makes it a potential candidate for water remediation applications.

Recently, in work reported by Zhuravlova et al. [52], the sulfur vacancies present on MoS₂ obtained by liquid-phase exfoliation were used to facilitate its functionalization with a specific receptor for Co²⁺, having a thiol termination (2,2':6',2''-terpyridine-4'-thiol). The modified sheets were deposited on SiO₂ to obtain films and then placed in a gold electrode system to develop an electrochemical Co²⁺ sensor. The structural properties of the functionalized MoS₂ film were obtained by means of SEM, XPS, and Raman spectroscopy. The thiol-functionalized MoS₂ film had an improved coverage compared to the film made of pristine MoS₂. Hence, the thiol functionalization worked as a cross-linker among MoS₂ adjacent layers. XPS analysis showed a decrease in the vacancy defects of thiol-functionalized MoS₂; this was evidence for the covalent functionalization of MoS₂ conducted on the sulfur vacancies. Raman spectra showed that the functionalization process does not destroy or alter the MoS₂ sheets. The sensor device was able to detect Co²⁺ from water with a limit detection of 1 ppm and was able to be selective towards Co²⁺ in the presence of K⁺, Ca²⁺, Mn²⁺, Cu²⁺, Cr³⁺, and Fe³⁺ (Figure 8). This work showed the facile functionalization of defective MoS₂ using the MoS₂ sulfur vacancies and a thiol end in the functional molecule. These results suggested that specific sensors can be created for detecting different heavy metals by just changing the receptor chemical properties.

Huang and collaborators [53] reported a sensor based on chitosan-functionalized MoSe₂ nanosheets to detect Hg²⁺ in water. The functionalized material was acquired through a single-step ionic liquid-assisted grinding method involving simultaneous exfoliation and functionalization. TEM and AFM analysis of the functionalized material demonstrated the obtention of mostly MoSe₂ single layers and a rough surface due to chitosan coating. The interaction between MoSe₂ and chitosan was monitored using FTIR spectroscopy. The sensing mechanism was based on the capability of Hg²⁺ ions to reduce chitosan using 3,3',5,5'-tetramethylbenzidine as a colorimetric indicator. The calibration curves were generated with the absorbance spectra; the limit of detection of this sensor was 3.5 nM Hg²⁺ (Figure 9). To validate the selectivity toward Hg²⁺ of the developed sensor, several cations and anions were tested in the colorimetric reaction in the presence and absence of Hg²⁺; the Hg²⁺ sample showed the highest absorbance at 652 nm and deep blue color compared with the other ions. Hence, the sensor developed by Huang et al. is selective and stable.

The tuning of chemical and mechanical surface characteristics in MoS₂ thin films through the application of diazonium chemistry was performed by Saha and colleagues in 2022 [54]. Aryl diazonium chemistry involving both electron-donating (4-tertbutyl) and electron-withdrawing (4-nitro) substituted groups was used to modify peroxide exfoliated MoS₂ films. SEM analysis of non-functionalized MoS₂ film revealed uniformly distributed multilayered sheets. In contrast, the functionalized MoS₂ films maintained a similar morphology, although some irregular features were observed, likely resulting from chemical surface modification. In this study, the degree of chemical interaction between distinct metal ions (Fe²⁺, Zn²⁺, Cu²⁺, and Co²⁺) and untreated and modified MoS₂ films was investigated. Untreated films were susceptible to interaction with specific metal ions, whereas the surfaces of the modified films were observed to be entirely passivated. These results indicate that the surface functionalization of TMDs with specific molecules, such as diazonium salts, can be an outstanding option to tune the selectivity of TMDs for the detection of specific metal ions.

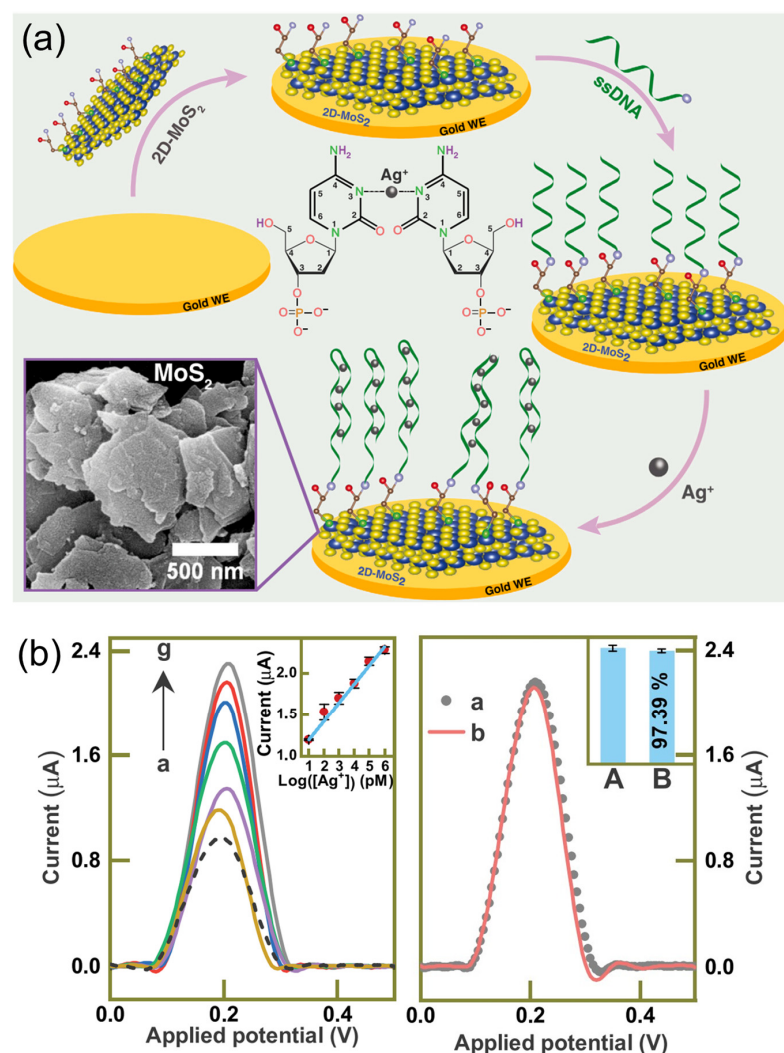


Figure 7. (a) Schematic representation of the Ag⁺ sensor reported by Pal and collaborators. The inset shows the FESEM image of COOH-MoS₂ nanosheets. (b) **Left.** Square wave voltammetry (SWV) response of the sensor developed by Pal and colleagues at various concentrations of Ag⁺ (Blank sample, 10 pM, 100 pM, 1 nM, 10 nM, 100 nM, 1 μM) (calibration curve as inset). **Right.** Re-usability performance (a, after; b, before) of the Ag⁺ sensor. The inset shows reusability after 6 months. Adapted from [51].

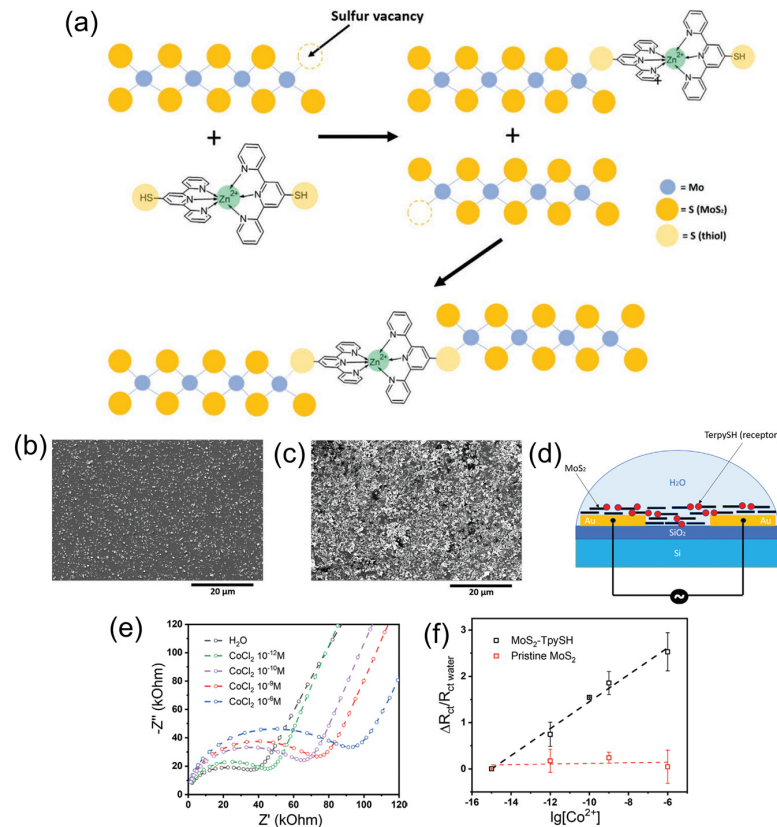


Figure 8. (a) Schematic representation of the functionalization of MoS₂ by repairing the sulfur vacancies with thiolate molecules. (b) SEM image of film made of pristine MoS₂. (c) SEM image of film made of thiol functionalized MoS₂. (d) Schematic representation of the fabricated sensor. (e) Electrochemical impedance spectroscopy (EIS) sensor response at various concentrations of Co²⁺. (f) Calibration curves of the sensors comparing pristine and functionalized MoS₂. Adapted from [52].

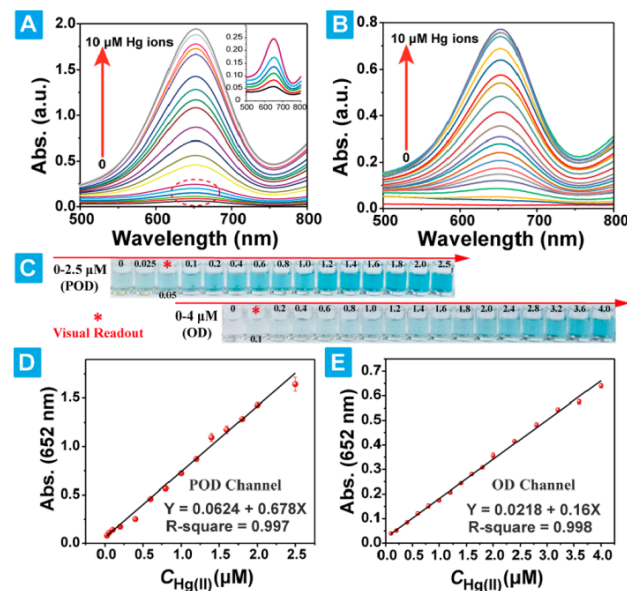


Figure 9. Colorimetric Hg²⁺ assay using CS-MoSe₂ nanosheets. (A,B) UV absorption spectra recorded for reaction systems containing Hg²⁺, CS-MoSe₂ NS, H₂O₂, and TMB at different concentrations. (C) Color changes in the reaction systems correlated with Hg²⁺ concentration. (D,E) Linear relationships between Hg²⁺ concentration and absorbance established based on the UV absorption spectra. Adapted from [53].

4. Gas Sensors

Atmospheric pollution is one of the biggest problems in environmental care. The development of highly sensitive and selective toxic gas sensors is an important goal to be achieved. In this direction, 2D-TMDs are promising materials to be used in gas sensors due to their high surface-to-volume ratio. The functionalization of 2D-TMDs with metal nanoparticles has been widely investigated because this type of functionalization has several effects on the sensing performance of these materials. Nanoparticles can exhibit the capability to alter the predominant type of charge carriers in TMDs, leading to distinct responses to molecules. Furthermore, nanoparticles increase the surface area of sensors, facilitating analyte diffusion, and they can also boost electron transfer between the sensor and analytes. Moreover, nanoparticles can also play a catalytic role in improving the dissociation and diffusion of analytes. Cho et al. [55] developed a volatile organic compound sensor based on MoS₂ functionalized with Au nanoparticles. First, MoS₂ nanosheets were obtained from liquid-phase exfoliation by sonicating MoS₂ powder. Then, Au nanoparticles were grown onto MoS₂ sheets. Monolayers and a few layers of MoS₂ were observed by TEM. Au nanoparticles grown on MoS₂ nanosheets had a diameter size lower than 10 nm. An Au-MoS₂ thin film was fabricated using vacuum filtration and located on the surface of a μ -electrode-printed substrate. The change in the resistance of Au-MoS₂ was measured while exposed to 100 ppm of VOC analytes such as toluene, hexane, ethanol, and acetone. The Au-MoS₂ sensor, after exposure to the analytes toluene and hexane, did not show an important change in the resistance. Conversely, the sensor showed the best response to the sensing of acetone. The most interesting feature of this report relies on the observed change of response of Au-MoS₂ to different VOCs depending on the sensing molecule. This feature was related to the change of the MoS₂ charge transfer type from p-type in pristine MoS₂ to n-type in Au-MoS₂.

Likewise, Bhardwaj and collaborators [56] functionalized MoS₂ with noble metal nanoparticles to be used as active materials in the detection of VOCs. In this work, MoS₂ nanosheets were grown directly on cellulose using the hydrothermal method. Au, Pd, and Pt were deposited on MoS₂ using a spray coating method. MoS₂ showed a micro-flower morphology, whereas Au nanoparticles with an average diameter size of 12 nm were observed to cover completely the surface of MoS₂. Pd and Pt nanoparticles had average diameters of 54 nm and 77 nm, respectively. Pd and Pt nanoparticles had a wide separation in MoS₂ nanosheets. The gas sensor performance of the functionalized MoS₂ was carried out at 50 °C with seven different VOCs at various ppm concentrations. The nanoparticle functionalized sensors showed an increment in the sensing response compared to pristine MoS₂, and Au-MoS₂ showed a better response to the lowest concentration of acetone. The use of cellulose as substrate provided stable baseline resistances and less sensitivity to humidity. Chacko et al. [57] reported a gas sensor based on MoS₂ functionalized with metals, specifically nickel and palladium. The metal functionalization was carried out by adding the metal precursors during the hydrothermal synthesis of MoS₂ to obtain MoS₂-Ni and MoS₂-Pd. The MoS₂ nanosheets exhibit a curly-like morphology of assembled nanosheets in FESEM analysis; this arrangement indicates a high surface area, which is important for good sensing performance. The metal-MoS₂ nanosheets were deposited on silicon wafer sensing devices and tested for different toxic and hazardous gases such as NH₃, H₂S, NO, and NO₂. It was observed that Ni-MoS₂ sensors demonstrated heightened sensitivity in detecting H₂S gas. Meanwhile, the Pd-MoS₂ sensor displayed exceptional sensitivity, stability, and notable selectivity in detecting NO. These high sensitivities are linked to the interaction between the metals with gas molecules and the synergy with the high surface area of MoS₂ sheets. In the same direction, Lee and colleagues [58] reported in 2022 the functionalization of MoS₂ nanosheets with Pt-nanoparticles to improve its gas sensing performance toward H₂. In this work, CVD-grown MoS₂ was first functionalized with oxygen using O₂ plasma functionalization; then, Pt nanoparticles were grown through atomic layer deposition. Through AFM analysis, it was determined the obtention of ~eight-layer MoS₂ and that the oxidation process did not induce damage in the MoS₂

structure. The Pt nanoparticles were grown more homogeneously on the surface of oxygen-functionalized MoS₂, and they showed an island type grown in pristine MoS₂. The oxygen groups worked as nucleation sites for the formation of Pt nanoparticles homogeneously on the MoS₂ surface. The sensor device was fabricated by deposition of Cr/Au electrodes on the Pt-functionalized MoS₂ using e-beam evaporation (Figure 10). The sensor presented by Lee exhibited a reduction in its resistance when exposed to H₂. The sensor demonstrated a significant relative resistance change, exceeding 400 times the initial resistance, with a detection limit for H₂ set at 2.5 ppm.

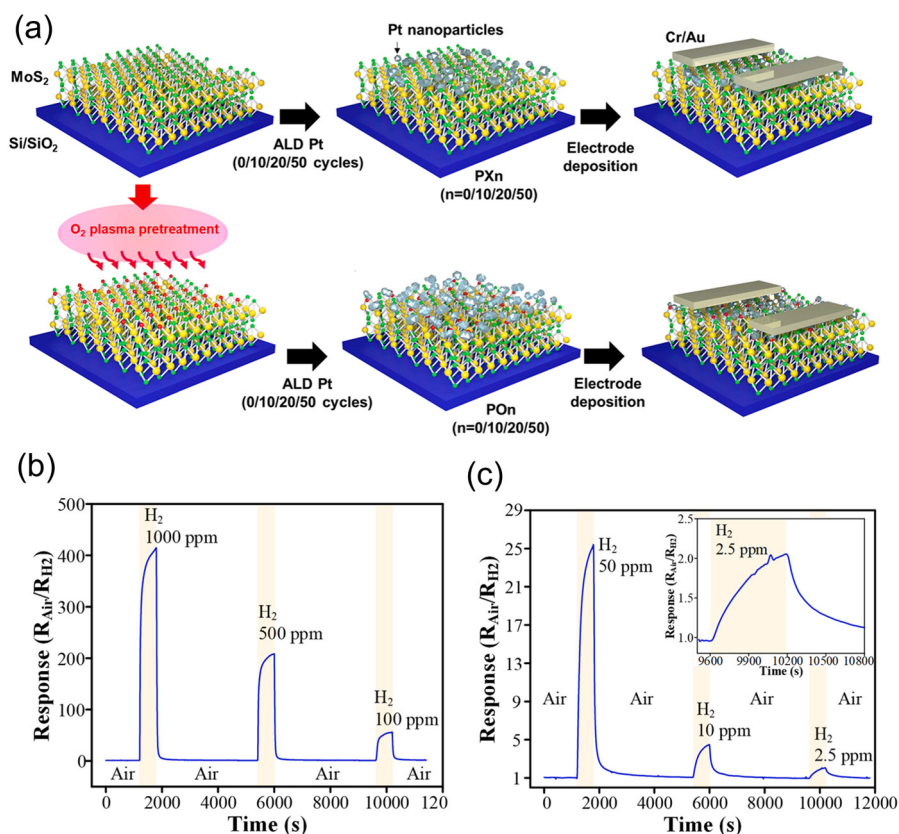


Figure 10. (a) Schematic representation of the fabrication process for the Pt-MoS₂ H₂ sensor. (b) Response of the Pt-MoS₂ sensor on exposure to hydrogen at various concentrations from 1000 ppm to 100 ppm. (c) Response of the Pt-MoS₂ H₂ sensor on exposure to hydrogen at various concentrations from 50 ppm to 2.5 ppm. Adapted from [58].

Other metal particle functionalized 2D-TMDs have been evaluated as gas sensors. The doping of WSe₂ with noble metals such as Pd, Ag, Au, and Pt was evaluated as a versatile approach to improve toxic gas sensing of CO₂, NO₂, and SO₂. Adsorption energy, band structure, and charge transfer were computed using first-principles density functional theory, finding that NO₂ adsorption on Ag-WSe₂ was the most energetically stable configuration, advising the development of an efficient NO₂ gas sensor [59]. The functionalization of WS₂ with Ag nanowires to improve their sensing performance towards NO₂ and acetone was reported by Yong Ko et al. [60]. Large layers (4 inches) of WS₂ were obtained by atomic layer deposition on an 8-inch SiO₂ wafer; with this technique, the number of WS₂ layers can be controlled, and one-, two- and four-layer WS₂ films were obtained. Then, Ag nanowires (AgNWs) were deposited on the WS₂ layer using spin coating. AgNWs coverage was found to be 2.5% of the total area of the WS₂ nanosheet. Finally, for the sensor device fabrication, Cr/Au electrodes were deposited on the surface of WS₂. The sensing performance of four-layer WS₂ was better for the detection of acetone and NO₂ compared to one-layer WS₂, which has an unobservable response. The authors compared the sensing performance of pristine and modified WS₂, observing that functionalized AgNWs-four-layer-WS₂ increases

by 667% its response to NO_2 molecules. On the other hand, Kim and collaborators [61] reported a sensor based on WS_2 functionalized with gold nanoparticles. Au nanoparticles were grown by photoreduction on WS_2 layers and deposited on polyamide as a substrate. Au nanoparticles with diameters of ~ 7.4 nm were obtained on the surface of WS_2 when irradiated 15 s with UV light. The sensors were reported to be flexible with high stability and present a good selectivity towards CO gas molecules with a sensor response of 1.48 (ratio of resistance in air and resistance in the presence of 50 ppm CO) (Figure 11). Likewise, Zhang and collaborators [62] developed a CO sensor based on Pd nanoparticles functionalized WSe_2 . Films of Pt- WSe_2 were prepared using the hydrothermal method. From SEM analysis, it can be observed that WSe_2 exhibits hexagonal nanosheet morphology and, in contrast to pristine WSe_2 , the Pd- WSe_2 composite displays a surface with increased roughness. In addition, the Pd particles are clustered in the form of small spheres on the WSe_2 surface. The dispersion of Pd- WSe_2 was applied to a sensor device through spray-coating, with Al_2O_3 serving as the substrate and Pt as the electrode. The Pd- WSe_2 thin film sensor exhibited outstanding sensing capabilities for CO gas molecules with a relative response of 15% and a detection limit of 1 ppm. Similarly, Sakhuja et al. [63] functionalized WSe_2 with metal nanoparticles to evaluate its performance as a gas sensor. In this case, Au and Pt nanoparticles were grown on the WSe_2 surface by metal salts reduction. TEM analysis showed the layers of WSe_2 covered with small Au/Pt nanoparticles. As expected, the functionalization of WSe_2 improved its performance at sensing NO_2 molecules. Au- WSe_2 showed a response to NO_2 of 170% and a detection limit of 100 ppb.

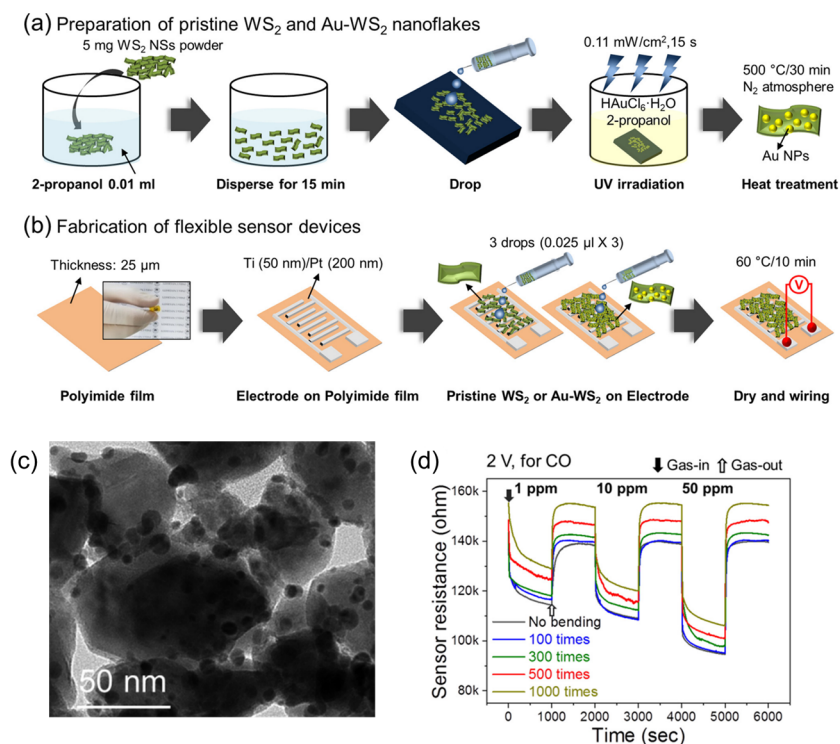


Figure 11. (a) Schematic illustration of the preparation procedures for unmodified and gold-functionalized WS_2 nanoflakes. (b) Construction of flexible gas sensors developed by Kim et al. (c) TEM image of Au- WS_2 nanoflakes. (d) Resistance curves of the Au-functionalized WS_2 gas sensor analyzed under two conditions: without bending and with bending at a radius of curvature of 4 mm, varying the number of bending cycles. Adapted from [61].

Most of the functionalization performed on MoS_2 for gas sensor applications implies its decoration with metal nanoparticles. However, other kinds of functionalization have also been tested. Kim and colleagues [64] fabricated a VOCs sensor based on MoS_2 functionalized with mercaptoundecanoic acid. The functionalization was corroborated

by XPS and FTIR analysis and was performed over the surface defects on MoS₂. The sensor developed by Kim et al. presented high sensitivity towards VOCs (toluene, hexane, ethanol, propanal, and acetone) with responses up to 15% for acetone and limiting concentrations down to 1 ppm. The advantage of functionalizing with thiol ligands instead of metal nanoparticles lies in the simplicity and high reproducibility of carrying out the thiol ligand functionalization.

Humidity sensors based on functionalized 2D-TDMs have been explored. In 2020, Gupta et al. [65] used a wet chemical method to generate WS₂ functionalized with Pt nanoparticles for the development of a humidity sensor. The Pt functionalization was confirmed by TEM showing small Pt particles decorating the layers of WS₂. HR-TEM images revealed interlayer spacings of 0.27 nm and 0.194 nm, which correspond to the (100) planes of WS₂ and Pt, respectively. The sensor device was prepared by drop-casting of Pt-WS₂ on Ti/Pt-based interdigitated electrodes and placed in a chamber with controlled humidity and temperature. The authors compared the sensor performance of pristine WS₂ with Pt-WS₂, observing that Pt-WS₂ increased its humidity response up to 105.1X higher than pristine WS₂. For pristine WS₂ nanosheets, the sensitivity was determined to be 16.5 per RH%. However, with the introduction of Pt-decoration, the sensitivity significantly escalated to 1792 per RH%. In the following year, Gupta and collaborators [66] reported similar work, with the difference being that the humidity sensor was now based on Au-WS₂. Au nanoparticles were well dispersed on the surface of WS₂ with diameters ranging from 5 to 10 nm. In this case, Au-WS₂ showed an enormous two orders of magnitude better humidity response than pristine WS₂. The response of untreated WS₂ devices ranged from 52 (at 25% relative humidity) to 1066 (at 75% relative humidity). In contrast, the response of the sensing device utilizing Au-functionalized WS₂ nanosheets exhibited a broader range, spanning from 31 (at 25% RH) to 70,018 (at 75% RH). From these results, it can be highlighted that the type of metal used for the functionalization of TMDs has an extremely relevant effect on its electrochemical properties.

5. Raman Sensors

Raman spectroscopy is a versatile strategy to sense diverse analytes. The intensity of the weak Raman signals can be amplified by several orders of magnitude while reducing fluorescence in the analytes using surface-enhanced Raman scattering (SERS) platforms. Supported noble metal nanoparticles are commonly used for this purpose. The 2D-TMDs have been recently studied as SERS substrates as their electronic properties can be modulated to induce charge polarization, one of the mechanisms used to explain SERS. MoS₂ has been used as a SERS substrate since charge transfer and dipole–dipole coupling occurs on the monolayer, processes responsible of Raman enhancement [67]. The 2D Janus MoSSe was used as a SERS substrate for detecting biomolecules. The Janus surface was prepared departing from MoSe₂, followed by a sulfurization process to obtain MoSSe. TEM images allowed the authors to observe that the triangular structure of the single-crystalline MoSe₂ monolayer sheets was maintained after the surface sulfurization. The Janus surface of MoSSe presented an out-of-plane dipole that polarized charges in biomolecules such as glucose and dopamine, enhancing their Raman signals up to 10⁵ [68]. N-doped, Ag nanoparticle decorated MoS₂ and WS₂ nanohybrids were used as fluorescence quenchers SERS substrates for the sensing of rhodamine B at concentrations as low as nM and later for the high sensitivity and reproducibility of polycyclic aromatic hydrocarbons such as pyrene, anthracene, and 2,3-dihydroxynaphthalene. The morphology of the decorated TMDs was observed by TEM microscopy, and the layered structure of MoS₂ and WS₂ was observed. Ag-nanoparticles in N-MoS₂ had an average diameter of 3.4 nm and 2.2 nm for N-WS₂. The Raman signals enhancement was attributed to charge transfer and dipole–dipole coupling [69]. Likewise, Singh and colleagues [70] reported the functionalization of MoS₂ nanosheets with Ag nanoparticles using a hydrothermal process; in this case, the Ag-MoS₂ sheets were used as SERS substrates for the detection of methylene blue. FESEM images showed the presence of spherical Ag nanoparticles with an average diameter of 35 nm

on the surface of MoS₂. This sensor presented an enhancement factor of 10⁷. The authors suggest that the combination of Ag and MoS₂ facilitates enhanced charge transfer mechanisms, thereby improving the SERS sensing performance. Au-WS₂ nanosheets were further functionalized with a specific aptamer to enhance the selectivity of a SERS sensor towards a cardiac marker myoglobin [71]. FESEM imaging showed the lamellar structures of WS₂ with lateral sizes ranging from 50 to 100 nm. These structures were functionalized with Au-nanoparticles with a diameter average size of 29 nm. This biosensor was able to detect myoglobin in the 10 f mL⁻¹ to 0.1 µg mL⁻¹ concentration range.

The identification of α-fetoprotein (AFP), a biomarker for hepatocellular carcinoma, was conducted utilizing MoS₂ modified with an antibody targeting AFP and Au-Ag core-shell nanoparticles attached to a secondary antibody, thus establishing a sandwich-type SERS sensor [72]. The Au-Ag nanoparticles had a cubic morphology and an average diameter of 58 nm. SEM analysis of the SERS substrates showed the layered structure of MoS₂ having micro-sized diameters and the cubic Au-Ag nanoparticles deposited on its surface. This platform was deposited on a silicon wafer and decorated with Ag-Au nanocubes to enhance the hot spots on the immunosensor (Figure 12). The newly designed SERS immunosensor demonstrated a broad linear detection span (ranging from 1 pg mL⁻¹ to 10 ng mL⁻¹) with an ultra-low limit of detection of 0.03 pg mL⁻¹.

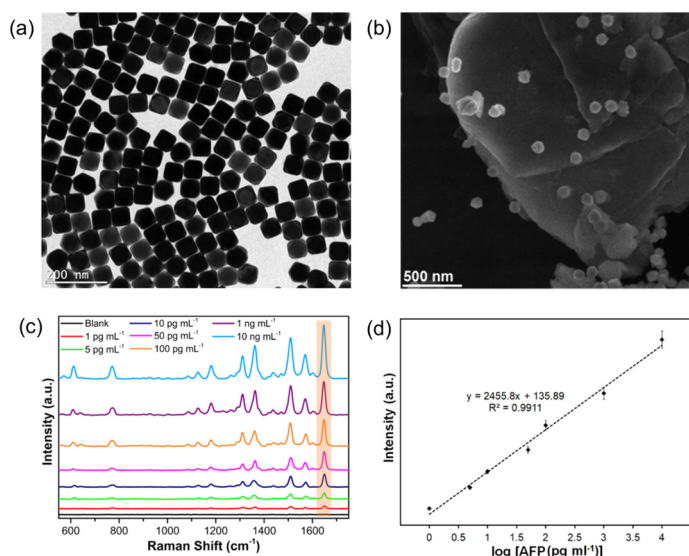


Figure 12. (a) TEM image of Au@Ag nanoparticles. (b) TEM image of Au@Ag-MoS₂ substrates. (c) SERS spectra of R6G at various concentrations of AFP. (d) Calibration curve of the sensor response. Adapted from [72].

To amplify the chemical enhancement in SERS of molecules deposited on metal nanoparticles functionalized 2D-TMDs, Photo-Induced Enhanced Raman Spectroscopy (PIERS) has been used; this technique leverages electron migration from semiconductors to metal nanoparticles triggered by UV light exposure. Abid et al. [73] used PIERS to enhance the sensing performance toward 4-mercaptobenzoic acid of AuNPs-WS₂. WS₂ layers had an average lateral size of 100 nm, and the gold nanoparticles had an average radius of 27 nm. The photo-activation of WS₂ results in a four-fold signal improvement compared to SERS from AuNPs-WS₂ without UV irradiation.

Besides metal nanoparticle functionalization, the 2D-TMDs functionalization with other constituents to improve their SERS performance was achieved. In 2020, MoS₂ was decorated with graphene-microflowers (GMFs) [74]. The MoS₂ platform had a flat surface with extensive internal corrugations, and individual GMFs had an average size of 2.25 µm. GMFs were effectively deposited onto the W-MoS₂ platform. These GMFs acted as molecular enhancers, generating SERS ‘active regions’. GMFs/W-MoS₂ showed an enhancement factor of 2.96 × 10⁷ for rhodamine B (Figure 13).

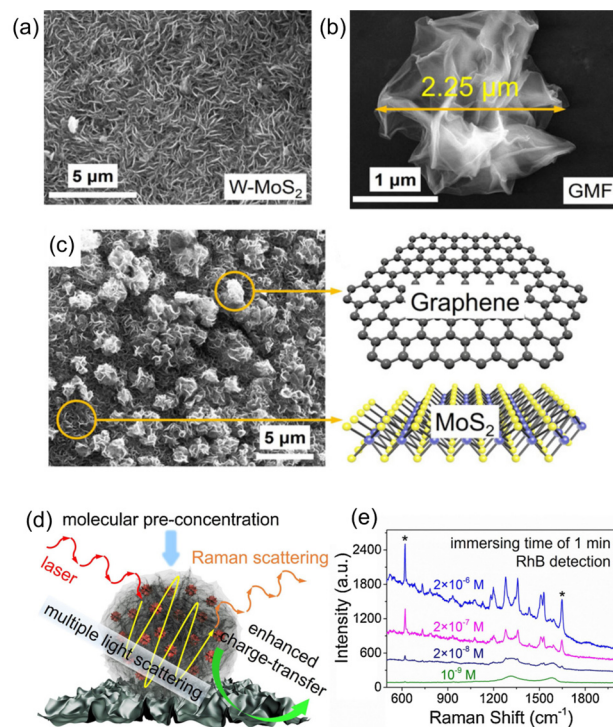


Figure 13. (a) SEM image of MoS₂. (b) SEM image of GMF. (c) SEM image of GMFs/MoS₂. (d) Schematic representation of SERS performance on GMFs/W-MoS₂. (e) Raman spectral profiles of RhB across various concentration levels. * denotes the principal vibrational modes of RhB. Adapted from [74].

6. Concluding Remarks and Perspectives

The 2D-TMDs are semiconductors with a bandgap in the visible to n-IR frequencies in the electromagnetic spectrum. The almost full d-orbitals in the electronic structure of 2D-TMDs allow the layer-dependent bandgaps tuning, electrostatic coupling, and photo switching, making them excellent materials for field-effect transistors (FETs), ultrasensitive sensors, flexible electronics, fluorescence quenchers, and Raman enhancers [75]. In addition, 2D-TMDs can be easily integrated into membranes by a simple vacuum filtration methodology, improving the sensing mechanism in microfluidic and nanofluidic systems [76]. The electrical properties and the chemical structure of 2D-TMDs allow the design and production of adaptable transducers for electrochemical, optical, electrical, and SERS detection, demonstrating great potential for the massive production of flexible and reliable sensors. The 2D-TMDs produced by chemical methodologies such as CVD, hydrothermal, and liquid-phase exfoliation present defects, vacancies, and dangling bonds facilitating chemical functionalization.

Functionalizing 2D-TMDs provides a versatile means to tune and regulate their surface properties, expanding their potential applications in chemical sensors. One area where surface functionalization of 2D-TMDs has a major impact is in increasing the detection sensibility by making them more selective. While 2D-TMDs functionalized with noble metal nanoparticles are the most widely nanohybrid material used for sensing, there is an increasing interest in exploring more versatile functionalization approaches, including functionalization with proteins, DNA, and polymers, which encompasses a broader spectrum of possibilities for tailoring the sensing properties of 2D-TMDs. However, the quest for increased sensory performance in 2D-TMDs requires further research aimed at identifying specific molecules for the functionalization of 2D-TMDs, depending on the device to be developed. These molecules, once attached to the surface of 2D-TMDs, offer the potential to improve the selectivity towards specific analytes. Addressing the selectivity challenge

by strategically functionalizing 2D-TMDs with molecules able to perform selectivity could pave the way toward highly specialized chemical sensors.

Finally, a crucial step is to subject the manufactured sensors to rigorous testing in samples and conditions that replicate real-world conditions. For example, evaluating sensors in human serum or blood for biomolecule detection, in polluted water for heavy metal detection, and in outdoor air for gas sensors. This practical application-oriented approach not only validates sensor performance, but also highlights the potential impact of 2D-TMDs in addressing critical challenges such as selectivity, sensibility, and stability.

Author Contributions: Writing original draft preparation S.A. and M.Q., reviewing and editing, S.A. and M.Q., funding acquisition, M.Q. All authors have read and agreed to the published version of the manuscript.

Funding: This research was funded by CONAHCYT through projects A1-S-8817 and 1564464. S.A. thanks to CONAHCYT for the postdoctoral fellowship 2023–2024.

Conflicts of Interest: The authors declare no conflicts of interest.

References

1. Chen, X.; Yao, C.; Li, Z. Microarray-Based Chemical Sensors and Biosensors: Fundamentals and Food Safety Applications. *TrAC Trends Anal. Chem.* **2023**, *158*, 116785. [[CrossRef](#)]
2. Kassal, P.; Steinberg, M.D.; Steinberg, I.M. Wireless Chemical Sensors and Biosensors: A Review. *Sens. Actuators B Chem.* **2018**, *266*, 228–245. [[CrossRef](#)]
3. McDonagh, C.; Burke, C.S.; MacCraith, B.D. Optical Chemical Sensors. *Chem. Rev.* **2008**, *108*, 400–422. [[CrossRef](#)] [[PubMed](#)]
4. Gai, L.Y.; Lai, R.P.; Dong, X.H.; Wu, X.; Luan, Q.T.; Wang, J.; Lin, H.F.; Ding, W.H.; Wu, G.L.; Xie, W.F. Recent Advances in Ethanol Gas Sensors Based on Metal Oxide Semiconductor Heterojunctions. *Rare Metals* **2022**, *41*, 1818–1842. [[CrossRef](#)]
5. Anichini, C.; Czepa, W.; Pakulski, D.; Aliprandi, A.; Ciesielski, A.; Samorì, P. Chemical Sensing with 2D Materials. *Chem. Soc. Rev.* **2018**, *47*, 4860–4908. [[CrossRef](#)] [[PubMed](#)]
6. Lee, C.W.; Suh, J.M.; Jang, H.W. Chemical Sensors Based on Two-Dimensional (2D) Materials for Selective Detection of Ions and Molecules in Liquid. *Front. Chem.* **2019**, *7*, 490901. [[CrossRef](#)]
7. Chhowalla, M.; Liu, Z.; Zhang, H. Two-Dimensional Transition Metal Dichalcogenide (TMD) Nanosheets. *Chem. Soc. Rev.* **2015**, *44*, 2584–2586. [[CrossRef](#)]
8. Splendiani, A.; Sun, L.; Zhang, Y.; Li, T.; Kim, J.; Chim, C.Y.; Galli, G.; Wang, F. Emerging Photoluminescence in Monolayer MoS₂. *Nano Lett.* **2010**, *10*, 1271–1275. [[CrossRef](#)]
9. Sulleiro, M.V.; Dominguez-Alfaro, A.; Alegret, N.; Silvestri, A.; Gómez, I.J. 2D Materials towards Sensing Technology: From Fundamentals to Applications. *Sens. Biosensing Res.* **2022**, *38*, 100540. [[CrossRef](#)]
10. Hassan, J.Z.; Raza, A.; Din Babar, Z.U.; Kumar, U.; Kaner, N.T.; Cassinese, A. 2D Material-Based Sensing Devices: An Update. *J. Mater. Chem. A Mater.* **2023**, *11*, 6016–6063. [[CrossRef](#)]
11. Llobet, E. Transition Metal Dichalcogenide Based Toxic Gas Sensing. *Curr. Opin. Environ. Sci. Health* **2024**, *37*, 100533. [[CrossRef](#)]
12. Gan, X.; Zhao, H.; Schirhagl, R.; Quan, X. Two-Dimensional Nanomaterial Based Sensors for Heavy Metal Ions. *Microchim. Acta* **2018**, *185*, 478. [[CrossRef](#)]
13. Neog, A.; Biswas, R. WS₂ Nanosheets as a Potential Candidate towards Sensing Heavy Metal Ions: A New Dimension of 2D Materials. *Mater. Res. Bull.* **2021**, *144*, 111471. [[CrossRef](#)]
14. Lei, Z.L.; Guo, B. 2D Material-Based Optical Biosensor: Status and Prospect. *Adv. Sci.* **2022**, *9*, 2102924. [[CrossRef](#)]
15. Li, S.; Ma, L.; Zhou, M.; Li, Y.; Xia, Y.; Fan, X.; Cheng, C.; Luo, H. New Opportunities for Emerging 2D Materials in Bioelectronics and Biosensors. *Curr. Opin. Biomed. Eng.* **2020**, *13*, 32–41. [[CrossRef](#)]
16. Yang, S.; Jiang, C.; Wei, S.H. Gas Sensing in 2D Materials. *Appl. Phys. Rev.* **2017**, *4*, 021304. [[CrossRef](#)]
17. Geronimo, I.; Lee, E.C.; Singh, N.J.; Kim, K.S. How Different Are Electron-Rich and Electron-Deficient π Interactions? *J. Chem. Theory Comput.* **2010**, *6*, 1931–1934. [[CrossRef](#)]
18. Lee, E.C.; Kim, D.; Jurečka, P.; Tarakeswarar, P.; Hobza, P.; Kim, K.S. Understanding of Assembly Phenomena by Aromatic–Aromatic Interactions: Benzene Dimer and the Substituted Systems. *J. Phys. Chem. A* **2007**, *111*, 3446–3457. [[CrossRef](#)] [[PubMed](#)]
19. Hunter, C.A.; Sanders, J.K.M. The Nature of π - π Interactions. *J. Am. Chem. Soc.* **1990**, *112*, 5525–5534. [[CrossRef](#)]
20. Jeong, J.H.; Kang, S.; Kim, N.; Joshi, R.; Lee, G.H. Recent Trends in Covalent Functionalization of 2D Materials. *Phys. Chem. Chem. Phys.* **2022**, *24*, 10684–10711. [[CrossRef](#)] [[PubMed](#)]
21. Varghese, S.S.; Varghese, S.H.; Swaminathan, S.; Singh, K.K.; Mittal, V. Two-Dimensional Materials for Sensing: Graphene and Beyond. *Electronics* **2015**, *4*, 651–687. [[CrossRef](#)]
22. Kumari, R.; Kumar, R. Review—Recent Advances in MoS₂ and Its Derivatives-Based Two-Dimensional Gas Sensors. *ECS J. Solid. State Sci. Technol.* **2022**, *11*, 097003. [[CrossRef](#)]

23. Huang, X.Y.; Chen, K.; Xie, W.; Li, Y.; Yang, F.; Deng, Y.; Li, J.; Jiang, F.; Shu, Y.; Wu, L.; et al. Chemiresistive Gas Sensors Based on Highly Permeable Sn-Doped Bismuth Subcarbonate Microspheres: Facile Synthesis, Sensing Performance, and Mechanism Study. *Adv. Funct. Mater.* **2023**, *33*, 2304718. [[CrossRef](#)]
24. Chia, H.L.; Mayorga-Martinez, C.C.; Pumera, M. Doping and Decorating 2D Materials for Biosensing: Benefits and Drawbacks. *Adv. Funct. Mater.* **2021**, *31*, 2102555. [[CrossRef](#)]
25. Daneshnia, S.; Adeli, M.; Yari, A.; Shams, A.; Donskyi, I.S.; Unger, W.E.S. Low Temperature Functionalization of Two-Dimensional Boron Nitride for Electrochemical Sensing. *Mater. Res. Express* **2019**, *6*, 095076. [[CrossRef](#)]
26. García-Miranda Ferrari, A.; Rowley-Neale, S.J.; Banks, C.E. Recent Advances in 2D Hexagonal Boron Nitride (2D-HBN) Applied as the Basis of Electrochemical Sensing Platforms. *Anal. Bioanal. Chem.* **2021**, *413*, 663–672. [[CrossRef](#)]
27. Ramanathan, A.A. Defect Functionalization of MoS₂ Nanostructures as Toxic Gas Sensors: A Review. *IOP Conf. Ser. Mater. Sci. Eng.* **2018**, *305*, 012001. [[CrossRef](#)]
28. Chou, S.S.; De, M.; Kim, J.; Byun, S.; Dykstra, C.; Yu, J.; Huang, J.; Dravid, V.P. Ligand Conjugation of Chemically Exfoliated MoS₂. *J. Am. Chem. Soc.* **2013**, *135*, 4584–4587. [[CrossRef](#)]
29. Huang, J.; Dong, Z.; Li, Y.; Li, J.; Tang, W.; Yang, H.; Wang, J.; Bao, Y.; Jin, J.; Li, R. MoS₂ Nanosheet Functionalized with Cu Nanoparticles and Its Application for Glucose Detection. *Mater. Res. Bull.* **2013**, *48*, 4544–4547. [[CrossRef](#)]
30. Kong, R.M.; Ding, L.; Wang, Z.; You, J.; Qu, F. A Novel Aptamer-Functionalized MoS₂ Nanosheet Fluorescent Biosensor for Sensitive Detection of Prostate Specific Antigen. *Anal. Bioanal. Chem.* **2015**, *407*, 369–377.
31. Zhang, Y.; Feng, D.; Xu, Y.; Yin, Z.; Dou, W.; Habiba, U.E.; Pan, C.; Zhang, Z.; Mou, H.; Deng, H.; et al. DNA-Based Functionalization of Two-Dimensional MoS₂ FET Biosensor for Ultrasensitive Detection of PSA. *Appl. Surf. Sci.* **2021**, *548*, 149169. [[CrossRef](#)]
32. Lin, K.C.; Jagannath, B.; Muthukumar, S.; Prasad, S. Sub-Picomolar Label-Free Detection of Thrombin Using Electrochemical Impedance Spectroscopy of Aptamer-Functionalized MoS₂. *Analyst* **2017**, *142*, 2770–2780. [[CrossRef](#)]
33. Behera, P.; Singh, K.K.; Pandit, S.; Saha, D.; Saini, D.K.; De, M. Machine Learning-Assisted Array-Based Detection of Proteins in Serum Using Functionalized MoS₂ Nanosheets and Green Fluorescent Protein Conjugates. *ACS Appl. Nano Mater.* **2021**, *4*, 3843–3851. [[CrossRef](#)]
34. Xu, B.; Su, Y.; Li, L.; Liu, R.; Lv, Y. Thiol-Functionalized Single-Layered MoS₂ Nanosheet as a Photoluminescence Sensing Platform via Charge Transfer for Dopamine Detection. *Sens. Actuators B Chem.* **2017**, *246*, 380–388. [[CrossRef](#)]
35. Guo, Y.; Shu, Y.; Li, A.; Li, B.; Pi, J.; Cai, J.; Cai, H.H.; Gao, Q. Efficient Electrochemical Detection of Cancer Cells on in Situ Surface-Functionalized MoS₂ Nanosheets. *J. Mater. Chem. B* **2017**, *5*, 5532–5538. [[CrossRef](#)]
36. Singh, C.; Ali, M.A.; Kumar, V.; Ahmad, R.; Sumana, G. Functionalized MoS₂ Nanosheets Assembled Microfluidic Immunosensor for Highly Sensitive Detection of Food Pathogen. *Sens. Actuators B Chem.* **2018**, *259*, 1090–1098. [[CrossRef](#)]
37. Zhang, W.; Yang, J.; Wu, D. Surface-Functionalized MoS₂ Nanosheets Sensor for Direct Electrochemical Detection of PIK3CA Gene Related to Lung Cancer. *J. Electrochem. Soc.* **2020**, *167*, 027501. [[CrossRef](#)]
38. Alagh, A.; Annanouch, F.E.; Llobet, E. Enhanced Gas Sensing Characteristics of Metal Doped WS₂ nanoflowers. *Proc. IEEE Sens.* **2021**, *2021*, 1–4. [[CrossRef](#)]
39. Annanouch, F.E.; Malik, S.B.; Alagh, A.; Llobet, E. High-Performance DMMP Gas Sensor Using PtO/WS₂ Hybrid Nanosheets. *Proc. IEEE Sens.* **2023**, *2023*, 1–4. [[CrossRef](#)]
40. Wang, X.; Deng, W.; Shen, L.; Yan, M.; Ge, S.; Yu, J. A Sensitive Quenched Electrochemiluminescent DNA Sensor Based on the Catalytic Activity of Gold Nanoparticle Functionalized MoS₂. *New J. Chem.* **2015**, *39*, 8100–8107. [[CrossRef](#)]
41. Xiao, H.; Cao, L.; Qin, H.; Wei, S.; Gu, M.; Zhao, F.; Chen, Z. Non-Enzymatic Lactic Acid Sensor Based on AuPtNPs Functionalized MoS₂ Nanosheet as Electrode Modified Materials. *J. Electroanal. Chem.* **2021**, *903*, 115806. [[CrossRef](#)]
42. Zhu, D.; Liu, W.; Zhao, D.; Hao, Q.; Li, J.; Huang, J.; Shi, J.; Chao, J.; Su, S.; Wang, L. Label-Free Electrochemical Sensing Platform for MicroRNA-21 Detection Using Thionine and Gold Nanoparticles Co-Functionalized MoS₂ Nanosheet. *ACS Appl. Mater. Interfaces* **2017**, *9*, 35597–35603. [[CrossRef](#)]
43. Quintana, M. 2D Materials and van Der Waals Heterostructures Platforms for Advanced Sensing of COVID-19. In *Biomedical Innovations to Combat COVID-19*; Academic Press: Cambridge, MA, USA, 2022; pp. 241–252. [[CrossRef](#)]
44. Peng, X.; Zhou, Y.; Nie, K.; Zhou, F.; Yuan, Y.; Song, J.; Qu, J. Promising Near-Infrared Plasmonic Biosensor Employed for Specific Detection of SARS-CoV-2 and Its Spike Glycoprotein. *New J. Phys.* **2020**, *22*, 103046. [[CrossRef](#)]
45. Chen, Q.; Chen, J.; Gao, C.; Zhang, M.; Chen, J.; Qiu, H. Hemin-Functionalized WS₂ Nanosheets as Highly Active Peroxidase Mimetics for Label-Free Colorimetric Detection of H₂O₂ and Glucose. *Analyst* **2015**, *140*, 2857–2863. [[CrossRef](#)]
46. Yang, J.K.; Lee, H.R.; Hwang, I.J.; Kim, H.I.; Bin Yim, D.; Kim, J.H. Fluorescent 2D WS₂ Nanosheets Bearing Chemical Affinity Elements for the Recognition of Glycated Hemoglobin. *Adv. Heal. Mater.* **2018**, *7*, 1701496. [[CrossRef](#)]
47. Luo, Y.; Wu, D.; Li, Z.; Li, X.Y.; Wu, Y.; Feng, S.P.; Menon, C.; Chen, H.; Chu, P.K. Plasma Functionalized MoSe₂ for Efficient Nonenzymatic Sensing of Hydrogen Peroxide in Ultra-Wide PH Range. *SmartMat* **2022**, *3*, 491–502. [[CrossRef](#)]
48. Song, Y.; Yan, X.; Ostermeyer, G.; Li, S.; Qu, L.; Du, D.; Li, Z.; Lin, Y. Direct Cytosolic MicroRNA Detection Using Single-Layer Perfluorinated Tungsten Diselenide Nanoplatform. *Anal. Chem.* **2018**, *90*, 10369–10376. [[CrossRef](#)] [[PubMed](#)]
49. Gan, X.; Zhao, H.; Wong, K.Y.; Lei, D.Y.; Zhang, Y.; Quan, X. Covalent Functionalization of MoS₂ Nanosheets Synthesized by Liquid Phase Exfoliation to Construct Electrochemical Sensors for Cd (II) Detection. *Talanta* **2018**, *182*, 38–48. [[CrossRef](#)] [[PubMed](#)]

50. Bazylewski, P.; Van Middelkoop, S.; Divigalpitiya, R.; Fanchini, G. Solid-State Chemiresistors from Two-Dimensional MoS₂ Nanosheets Functionalized with L-Cysteine for In-Line Sensing of Part-Per-Billion Cd²⁺ Ions in Drinking Water. *ACS Omega* **2020**, *5*, 643–649. [[CrossRef](#)] [[PubMed](#)]
51. Pal, C.; Kumar, A.; Majumder, S. Fabrication of SsDNA Functionalized MoS₂ Nanoflakes Based Label-Free Electrochemical Biosensor for Explicit Silver Ion Detection at Sub-Pico Molar Level. *Colloids Surf. A Physicochem. Eng. Asp.* **2022**, *655*, 130241. [[CrossRef](#)]
52. Zhuravlova, A.; Ricciardulli, A.G.; Pakulski, D.; Gorczyński, A.; Kelly, A.; Coleman, J.N.; Ciesielski, A.; Samorì, P. High Selectivity and Sensitivity in Chemiresistive Sensing of Co(II) Ions with Liquid-Phase Exfoliated Functionalized MoS₂: A Supramolecular Approach. *Small* **2023**, *19*, 2208100. [[CrossRef](#)]
53. Huang, L.; Zhu, Q.; Zhu, J.; Luo, L.; Pu, S.; Zhang, W.; Zhu, W.; Sun, J.; Wang, J. Portable Colorimetric Detection of Mercury(II) Based on a Non-Noble Metal Nanozyme with Tunable Activity. *Inorg. Chem.* **2019**, *58*, 1638–1646. [[CrossRef](#)] [[PubMed](#)]
54. Saha, D.; Angizi, S.; Darestani-Farahani, M.; Dalmieda, J.; Selvaganapathy, P.R.; Kruse, P. Tuning the Chemical and Mechanical Properties of Conductive MoS₂ Thin Films by Surface Modification with Aryl Diazonium Salts. *Langmuir* **2022**, *38*, 3666–3675. [[CrossRef](#)]
55. Cho, S.Y.; Koh, H.J.; Yoo, H.W.; Kim, J.S.; Jung, H.T. Tunable Volatile-Organic-Compound Sensor by Using Au Nanoparticle Incorporation on MoS₂. *ACS Sens.* **2017**, *2*, 183–189. [[CrossRef](#)] [[PubMed](#)]
56. Bhardwaj, R.; Selamneni, V.; Thakur, U.N.; Sahatiya, P.; Hazra, A. Detection and Discrimination of Volatile Organic Compounds by Noble Metal Nanoparticle Functionalized MoS₂ Coated Biodegradable Paper Sensors. *New J. Chem.* **2020**, *44*, 16613–16625. [[CrossRef](#)]
57. Chacko, L.; Massera, E.; Aneesh, P.M. Enhancement in the Selectivity and Sensitivity of Ni and Pd Functionalized MoS₂ Toxic Gas Sensors. *J. Electrochem. Soc.* **2020**, *167*, 106506. [[CrossRef](#)]
58. Lee, S.; Kang, Y.; Lee, J.; Kim, J.; Shin, J.W.; Sim, S.; Go, D.; Jo, E.; Kye, S.; Kim, J.; et al. Atomic Layer Deposited Pt Nanoparticles on Functionalized MoS₂ as Highly Sensitive H₂ Sensor. *Appl. Surf. Sci.* **2022**, *571*, 151256. [[CrossRef](#)]
59. Ni, J.; Wang, W.; Quintana, M.; Jia, F.; Song, S. Adsorption of Small Gas Molecules on Strained Monolayer WSe₂ Doped with Pd, Ag, Au, and Pt: A Computational Investigation. *Appl. Surf. Sci.* **2020**, *514*, 145911. [[CrossRef](#)]
60. Ko, K.Y.; Song, J.G.; Kim, Y.; Choi, T.; Shin, S.; Lee, C.W.; Lee, K.; Koo, J.; Lee, H.; Kim, J.; et al. Improvement of Gas-Sensing Performance of Large-Area Tungsten Disulfide Nanosheets by Surface Functionalization. *ACS Nano* **2016**, *10*, 9287–9296. [[CrossRef](#)]
61. Kim, J.H.; Mirzaei, A.; Kim, H.W.; Kim, S.S. Flexible and Low Power CO Gas Sensor with Au-Functionalized 2D WS₂ Nanoflakes. *Sens. Actuators B Chem.* **2020**, *313*, 128040. [[CrossRef](#)]
62. Zhang, D.; Wang, D.; Pan, W.; Tang, M.; Zhang, H. Construction and DFT Study of Pd Decorated WSe₂ Nanosheets for Highly Sensitive CO Detection at Room Temperature. *Sens. Actuators B Chem.* **2022**, *360*, 131634. [[CrossRef](#)]
63. Sakhuja, N.; Gupta, A.; Jha, R.; Bhat, N. Noble Metal Nanoparticle Decorated Tungsten Diselenide Nanosheets for Ultrasensitive Detection of NO₂ at Room Temperature. *J. Alloys Compd.* **2022**, *899*, 163166. [[CrossRef](#)]
64. Kim, J.S.; Yoo, H.W.; Choi, H.O.; Jung, H.T. Tunable Volatile Organic Compounds Sensor by Using Thiolated Ligand Conjugation on MoS₂. *Nano Lett.* **2014**, *14*, 5941–5947.
65. Gupta, A.; Sakhuja, N.; Jha, R.; Bhat, N. Giant Humidity Responsiveness of Platinum Functionalized WS₂ Nanosheet Based Chemiresistors. *Proc. IEEE Sens.* **2020**, *2020*, 1–4. [[CrossRef](#)]
66. Gupta, A.; Sakhuja, N.; Jha, R.K.; Bhat, N. Ultrasensitive Chemiresistive Humidity Sensor Based on Gold Functionalized WS₂ Nanosheets. *Sens. Actuators A Phys.* **2021**, *331*, 113008. [[CrossRef](#)]
67. Ling, X.; Fang, W.; Lee, Y.H.; Araujo, P.T.; Zhang, X.; Rodriguez-Nieva, J.F.; Lin, Y.; Zhang, J.; Kong, J.; Dresselhaus, M.S. Raman Enhancement Effect on Two-Dimensional Layered Materials: Graphene, h-BN and MoS₂. *Nano Lett.* **2014**, *14*, 3033–3040. [[CrossRef](#)]
68. Jia, S.; Bandyopadhyay, A.; Kumar, H.; Zhang, J.; Wang, W.; Zhai, T.; Shenoy, V.B.; Lou, J. Biomolecular Sensing by Surface-Enhanced Raman Scattering of Monolayer Janus Transition Metal Dichalcogenide. *Nanoscale* **2020**, *12*, 10723–10729. [[CrossRef](#)]
69. Koklioti, M.A.; Bittencourt, C.; Noirfalise, X.; Saucedo-Orozco, I.; Quintana, M.; Tagmatarchis, N. Nitrogen-Doped Silver-Nanoparticle-Decorated Transition-Metal Dichalcogenides as Surface-Enhanced Raman Scattering Substrates for Sensing Polycyclic Aromatic Hydrocarbons. *ACS Appl. Nano Mater.* **2018**, *1*, 3625–3635. [[CrossRef](#)]
70. Singh, J.; Soni, R.K.; Nguyen, D.D.; Kumar Gupta, V.; Nguyen-Tri, P. Enhanced Photocatalytic and SERS Performance of Ag Nanoparticles Functionalized MoS₂ Nanoflakes. *Chemosphere* **2023**, *339*, 139735. [[CrossRef](#)] [[PubMed](#)]
71. Shorie, M.; Kumar, V.; Kaur, H.; Singh, K.; Tomer, V.K.; Sabherwal, P. Plasmonic DNA Hotspots Made from Tungsten Disulfide Nanosheets and Gold Nanoparticles for Ultrasensitive Aptamer-Based SERS Detection of Myoglobin. *Microchim. Acta* **2018**, *185*, 158. [[CrossRef](#)] [[PubMed](#)]
72. Er, E.; Sanchez-Iglesias, A.; Silvestri, A.; Arnaiz, B.; Liz-Marzan, L.M.; Prato, M.; Criado, A. Metal Nanoparticles/MoS₂ Surface-Enhanced Raman Scattering-Based Sandwich Immunoassay for A-fetoprotein Detection. *ACS Appl. Mater. Interfaces* **2021**, *13*, 8823–8831. [[CrossRef](#)] [[PubMed](#)]
73. Abid, K.; Belkhir, N.H.; Jaber, S.B.; Zribi, R.; Donato, M.G.; Di Marco, G.; Gucciardi, P.G.; Neri, G.; Maàlej, R. Photoinduced Enhanced Raman Spectroscopy with Hybrid Au@WS₂ Nanosheets. *J. Phys. Chem. C* **2020**, *124*, 20350–20358. [[CrossRef](#)]

74. Qiu, H.; Wang, M.; Zhang, L.; Cao, M.; Ji, Y.; Kou, S.; Dou, J.; Sun, X.; Yang, Z. Wrinkled 2H-Phase MoS₂ Sheet Decorated with Graphene-Microflowers for Ultrasensitive Molecular Sensing by Plasmon-Free SERS Enhancement. *Sens. Actuators B Chem.* **2020**, *320*, 128445. [[CrossRef](#)]
75. Schmidt, H.; Giustiniano, F.; Eda, G. Electronic Transport Properties of Transition Metal Dichalcogenide Field-Effect Devices: Surface and Interface Effects. *Chem. Soc. Rev.* **2015**, *44*, 7715–7736. [[CrossRef](#)]
76. Acosta, S.; Ojeda-Galván, H.J.; Quintana, M. 2D Materials towards Energy Conversion Processes in Nanofluidics. *Phys. Chem. Chem. Phys.* **2023**, *25*, 24264–24277. [[CrossRef](#)]

Disclaimer/Publisher’s Note: The statements, opinions and data contained in all publications are solely those of the individual author(s) and contributor(s) and not of MDPI and/or the editor(s). MDPI and/or the editor(s) disclaim responsibility for any injury to people or property resulting from any ideas, methods, instructions or products referred to in the content.